# Magnetoresistance oscillations in MBE-grown $Sb_2Te_3$ thin films

C. Weyrich, T. Merzenich, J. Kampmeier, I. E. Batov, G. Mussler, J. Schubert, D. Grützmacher, and Th. Schäpers

Citation: Appl. Phys. Lett. **110**, 092104 (2017); doi: 10.1063/1.4977848

View online: http://dx.doi.org/10.1063/1.4977848

View Table of Contents: http://aip.scitation.org/toc/apl/110/9

Published by the American Institute of Physics

# Magnetoresistance oscillations in MBE-grown $Sb_2Te_3$ thin films

C. Weyrich,[1,2,a)] T. Merzenich,[1,2] J. Kampmeier,[1,2] I. E. Batov,[1] G. Mussler,[1,2] J. Schubert,[1] D. Grützmacher,[1,2] and Th. Schäpers[1,2]
[1]*Peter Grünberg Institute (PGI-9) and JARA-Fundamentals of Future Information Technology, Forschungszentrum Jülich GmbH, 52425 Jülich, Germany*
[2]*Helmholtz Virtual Institute for Topological Insulators (VITI), Forschungszentrum Jülich, 52425 Jülich, Germany*

(Received 22 December 2016; accepted 17 February 2017; published online 2 March 2017)

We report on the Shubnikov–de Haas oscillations in the longitudinal resistance of thin films of three-dimensional topological insulator $Sb_2Te_3$ grown by means of molecular beam epitaxy. The oscillations persist up to the temperatures of 30 K, and the measurements at various tilt angles reveal that they originate from a two-dimensional system. Using a top gate, we further study the change of oscillation amplitude and frequency, which in combination with the standard Hall measurements suggest the origin of oscillations to be at the interface between the film and the Si substrate. *Published by AIP Publishing.* [http://dx.doi.org/10.1063/1.4977848]

Three dimensional topological insulators (TI) make up a new class of materials that are predicted to host metallic surface states enclosing an insulating bulk and a Dirac like linear energy dispersion located within the bulk band gap.[1–3] Therefore, charge carriers with a high mobility at the surface of these materials can be expected. Intriguing properties like spin–momentum locking and robustness against perturbations have made these surface states promising candidates for the future information technology and spintronic applications.[2–4] Especially, the prediction to host Majorana fermions in hybrid systems with superconductors[5,6] is particularly interesting for quantum computing and has further pushed research on these materials. However, all properties mentioned above are solely restricted to the topological protected surface states and thus require the bulk to be insulating in order to observe these effects in electrical transport. Otherwise, they will be masked by the bulk conductance. This has proven to be a difficult task since all the binary materials tend to be intrinsically doped due to the formation of crystal defects during growth.[7,8] Locating the conducting channels in transport measurements has thus been a prime task that will be addressed in this work. The Shubnikov–de Haas (SdH) oscillations pose a way to partially circumvent the influence of the bulk. If the mobility of surface state carriers is sufficiently high compared to bulk carriers, then the observation of SdH-oscillations on top of the bulk background signal is feasible. A previous theory states that the Dirac like nature of surface carriers becomes apparent in the quantization of Landau levels by shifting the filling factor in the quantum limit ($1/B \rightarrow 0$) from 0 to 1/2 due to the $\pi$-Berry phase.[9] In other words, by comparing the eigenvalues of the Hamilton operators of a classical electron gas $E_n = \hbar\omega_c(n + 1/2)$ and those of a Dirac system $E_n = v_F\sqrt{2e\hbar Bn}$ with $n$ denoting the energy level, the Fermi velocity $v_F$ and the cyclotron frequency, $\omega_c = eB/m_c$ where $m_c$ is the cyclotron mass and $B$ is the magnetic field. These levels align with the Fermi energy $E_F$ whenever the following conditions are fulfilled: $n + 1/2 = m_cE_F/e\hbar B$ for the classic system and $n = E_F^2/v_F^2 2e\hbar B$ for the Dirac system. Thus, one should be able to identify the surface states by extrapolating the Landau level fan diagram to $1/B = 0\ \mathrm{T}^{-1}$. For a Dirac system, the intersection with the filling factors is shifted from 0 to 1/2. So far, the SdH oscillations have been observed in various material systems like $Bi_2Se_3$,[10–13] $Bi_2Te_3$,[14–16] $Bi_2Te_2Se$,[17,18] and $(Bi_{1-x}Sb_x)_2Se_3$.[19]

Here, we report our findings in p-type doped $Sb_2Te_3$, which is a promising TI, due to its relatively large band gap of $\sim$170 meV.[20] Also, its Dirac cone is free, i.e., it is not accompanied by bulk bands at the same energy as in the case of $Bi_2Te_3$ for example, where the cone is located inside a valence band pocket at the $\Gamma$-point.[21] This gives access to the Dirac point without intersecting any bulk bands with the Fermi level. Angle-resolved photo emission spectroscopy (ARPES) has already revealed that the surface states exhibit a single non-degenerate Dirac cone,[22] and Jiang *et al.*[23] were able to observe the Landau quantization as well as a linear energy dispersion of surface states in scanning tunneling microscopy on $Sb_2Te_3$ thin films grown by molecular beam epitaxy (MBE).

The 13.6 nm thick $Sb_2Te_3$ epilayer was grown by means of solid-source MBE on an Si(111) substrate. Details on the growth process and topography can be found in Ref. 24, except for slight differences regarding the temperatures of the substrate during growth (350 °C instead of 300 °C) as well as the Te-effusion cell (380 °C instead of 330 °C). The implications of these changes on the film and transport properties are discussed in the supplementary material. Hall bars with widths between 20 and 60 $\mu$m were fabricated by optical lithography and $Ar^+$ dry etching. For the top gates, a 100 nm thick layer of high-$k$ dielectric $LaLuO_3$ was deposited on top of the Hall bar structures via pulsed laser deposition. For the ohmic contacts as well as the top gate, a Ti/Au layer system was used.

The magnetotransport measurements were carried out at temperatures between 1.7 and 30 K in a $^4$He variable temperature insert cryostat. A magnetic field up to 16 T was oriented at different tilt angles $\theta$ with respect to the layer surface, and the measurements were performed in a four-terminal

[a)]Electronic mail: c.weyrich@fz-juelich.de

configuration using the standard lock-in technique with an AC current of $I = 1\,\mu$A. The voltage probes were separated by 150 or 300 $\mu$m.

The sample exhibits monotonic positive magnetoresistance over the entire field range (cf. Fig. 1) as well as a weak antilocalization feature at small fields of $B \lesssim 100$ mT manifesting itself as a cusplike dip in resistance around zero field (see upper inset). At $B = 0$ T, we find a sheet resistance of $R_\square = 105\ \Omega$ and the standard Hall measurements reveal a hole concentration of the order of $n^{bulk} = 5 \times 10^{13}\,\mathrm{cm}^{-2}$ from a fit to the low field slope. These measurements yield a mobility of $\mu \approx 1000\,\mathrm{cm}^2/\mathrm{Vs}$ which is more than twice as high as found in an earlier work by Takagaki *et al.*[25] for MBE-grown $Sb_2Te_3$ on Si(111), who also did not observe any oscillations in their signal.

Unlike them, we observe that the Hall resistance $R_{yx}$ is slightly nonlinear at higher fields, revealing the influence of a second transport channel in parallel, as can be seen in Fig. 2. When the top gate voltage is swept from $V_g = -10$ V to more positive values, the slope of $R_{yx}$ increases. From the low field signal, we can evaluate that the hole concentration decreases from 6.8 to 4.5 $\times 10^{13}\,\mathrm{cm}^{-2}$ by increasing $V_g$ from $-10$ V to $+10$ V. This is a change of $\sim$20% compared to $V_g = 0$ V. The carrier concentrations extracted from $R_{yx}$ are shown as blue dots in the inset. By further looking at the gate dependence of our sheet resistance (Fig. 1, right inset), which does not feature a maximum within the accessible gate range, we find a clear indication that the Fermi level most likely cuts the valence band and cannot be tuned into the bulk band gap by applying a positive gate voltage.

The quantum oscillations of a 30 $\mu$m wide sample after subtracting a smooth background (see supplementary material for details) are shown in Fig. 3(a). Despite the low ratio between the background and the oscillating part of the signal, we can identify five extrema starting at $B = 8.5$ T. With the Onsager relation $F = e/2n^{SdH}\pi\hbar$, where $F$ is the period of the SdH-oscillations in $1/B$ for nonspin degenerate systems, we obtain a carrier concentration $n^{SdH} = 9.85 \times 10^{11}\,\mathrm{cm}^{-2}$ using

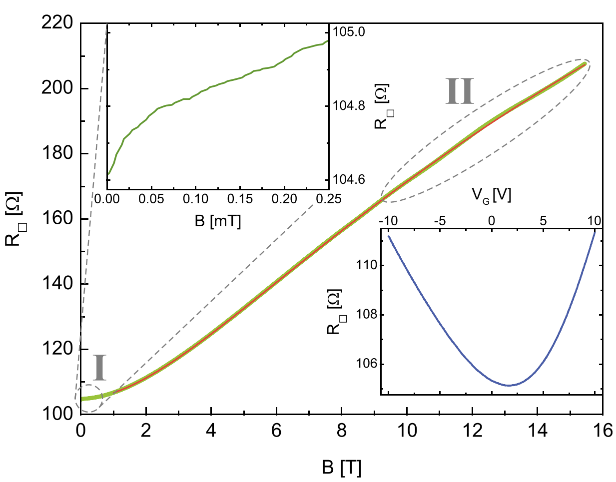


FIG. 1. Sheet resistance (green) and the smooth background (red) that was used to extract the superimposed oscillations. The upper left inset shows the weak antilocalization feature at fields below 100 mT, marked as region **I**. An emphasis on the high field part above 9 T (region **II**) reveals that the oscillations are weak but still visible in the raw data. In the lower right inset, $R_\square$ is plotted when sweeping the gate between $V_g = \pm 10$ V.

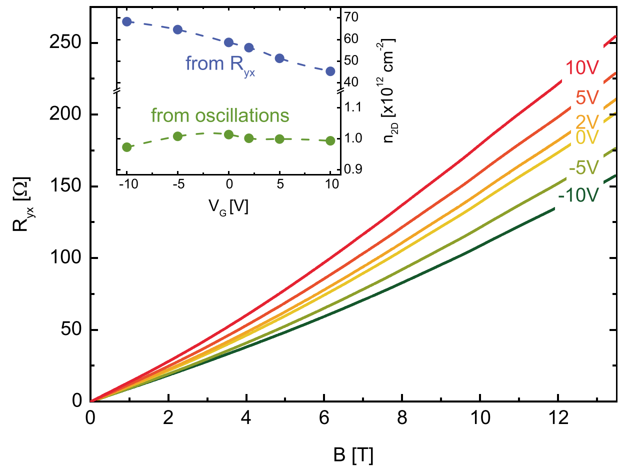


FIG. 2. Transversal resistance ($R_{yx}$) at different gate voltages. The inset shows the carrier concentrations calculated from the Hall measurements (blue) and from quantum oscillations (green). It is clearly visible that both methods show obvious differences in magnitudes as well as gate dependence.

the oscillation frequency of $1/F = 40.7$ T from the Fourier analysis. This is more than one order of magnitude below the values from Hall measurements. Together with the indication of multi-channel transport given by the nonlinearity of $R_{yx}$, we conclude that the oscillations originate from a transport channel that is at least partially separated from the bulk. If we plot the positions of the extrema in the Landau level index plot (cf. Fig. 3(b)), the extrapolation intersects at a level index of about 0.15, clearly different from the expected values of 0 for a classical two-dimensional electron gas as well as 1/2 for ideal Dirac fermions. This kind of shift has already been reported for many systems, and there are several studies discussing its origin. The most common explanations include a deviation of the Dirac spectrum from a strict linear dispersion due to strong spin–orbit coupling and lack of inversion symmetry of the surface states as well as a mixed system of normal and Dirac fermions.[26–28] These would lead to the Zeeman coupling of the carriers to the external magnetic field and a field dependence of the phase shift of the oscillations $\gamma$ according to $\Delta R_{xx} \sim \cos\left[2\pi(F/B - \gamma)\right]$. This gives rise to a nonlinearity in the Landau level index plot towards higher

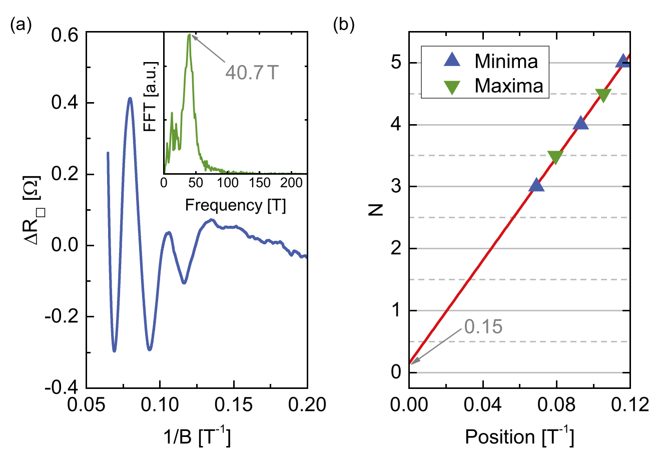


FIG. 3. (a) SdH-oscillations up to 15.5 T at 2 K and $V_g = 2$ V. From the fast Fourier spectrum (shown in the inset), we extract a frequency of 40.7 T. (b) The fan diagram where $N$ is the number of occupied Landau levels.

fields, which depends on the effective mass, Fermi velocity and g-factor of the charge carriers. The mixed system is further discussed in the supplementary material.

Oscillations can be observed up to the temperatures of 30 K, as shown in Fig. 4. Above this temperature, the signal becomes masked by noise. From the temperature dependence of the oscillation amplitude at fixed fields, the cyclotron mass $m_c$ of the charge carries can be found using the temperature damping term[29]

$$R_T = 2\pi^2 \frac{k_B T}{\hbar\omega_c} \bigg/ \sinh\left(2\pi^2 \frac{k_B T}{\hbar\omega_c}\right). \quad (1)$$

Here, $m_c$ is included in the cyclotron frequency $\omega_c$. As shown in the inset, this analysis has been performed for the first two extrema. We obtain $m_c/m_e = 0.081$ for the first maximum and $m_c/m_e = 0.078$ for the first minimum, with the free electron mass $m_e$. Both values are in good agreement with each other despite the small SdH-signal.

Fig. 5(a) shows quantum oscillations measured at varying angles plotted against the component of the field $B_\perp$ that is perpendicular to the plane of the sample. It is obvious that the frequency of the oscillations only depends on $B_\perp$ which verifies the two-dimensional nature of the system. If we assume a linear energy dispersion for the oscillating channel, then we can estimate the Fermi velocity $v_F$ from $n^{SdH}$ and $m_c$ obtained from the SdH-oscillations by differentiating the dispersion relation $E = v_F \hbar k$ as well as using the generalized definition of the cyclotron mass $m_c = k\hbar^2(\partial E/\partial k)^{-1}$[30] and the Fermi wave vector $k_F = \sqrt{4\pi n^{SdH}}$. This yields $v_F \approx 5 \times 10^5$ m/s that is in very good agreement with the value of the group velocity of the Dirac cone extracted from ARPES measurements by Plucinski *et al.*[20] From the oscillation frequency of the Dirac system ($E_F^2/v_F^2 2e\hbar = 40.7$ T), we can further obtain the Fermi energy $E_F \approx 118$ meV. Comparing this value to the same ARPES data, we can conclude that this value is sufficient to reach the valence band when coming from the Dirac point, which they estimated to be located about 85 meV above the valence band edge. Our values also agree well with the findings of Yoshimi *et al.*[31] who were

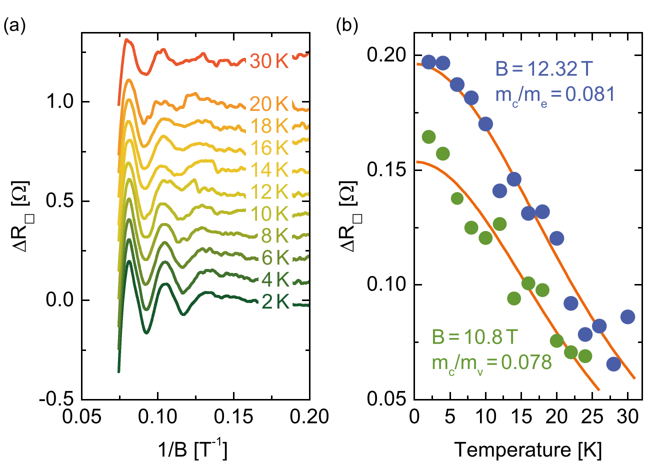


FIG. 4. (a) Temperature dependence of the oscillations up to 30 K (curves are shifted for clarity). (b) Fits to the temperature dependent amplitudes at the fixed field values $B = 12.3$ T (1st maximum) and $B = 10.8$ T (1st minimum).

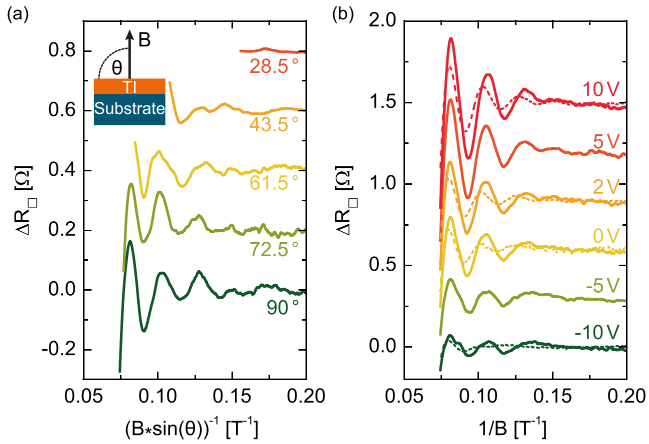


FIG. 5. (a) SdH-oscillations up to 13.5 T for different tilt angles $\theta$ of the magnetic field, plotted against the component of $B$ perpendicular to the sample surface. The inset depicts the definition of $\theta$. (b) Oscillations at various gate voltages for two different samples (solid and dashed lines) of same dimensions. While there are subtle differences in amplitude and frequency, both samples display the same qualitative behaviour. The amplitude increases when applying more positive gate voltages, whereas the frequency (and thus the carrier concentration) is almost unaffected. All curves are shifted for clarity.

able to probe the interface states between the MBE-grown $(Bi_{1-x}Sb_x)_2Te_3$ films and an InP(111) substrate using resonant tunneling spectroscopy. For $x = 1$, they estimate $v_F \approx 4 - 6 \times 10^5$ m/s, depending on the position relative to the Dirac point, which they calculate to be about 80 meV above the valence band.

Finally, we examine the effect of the top gate on the oscillation frequency and amplitude. Surprisingly, the former is hardly affected when $V_g$ is changed, as can be seen in Fig. 5(b), meaning that the carrier concentration remains unchanged. This is in contrast to the Hall measurements shown before, where the slope clearly shifts with the gate voltage. The straightforward explanation is such that the SdH-channel is located at the bottom interface of the film and therefore shielded from the top gate by the bulk. Given the fact that no second frequency can be observed, it appears that the top interface does not give rise to oscillations since it would be altered strongly by the top gate. This could be caused by oxidation of the surface during ex situ processing or band bending due to the dielectric. Another intriguing observation is the strong increase of oscillation amplitude when the gate is driven to more positive voltages. Since the bulk carrier concentration decreases too, one might relate this to the fact that the oscillations become more prominent if the background signal is reduced. Since the oscillating channel is shunted by the bulk, increasing the resistance of the bulk would drive more carriers into the SdH-system. However, from the lower inset in Fig. 1, it is obvious that the total sheet resistance increases only by about 5.5% going to the maximum gate voltages, and the change is rather symmetric with regard to $V_g = 0$ V. Therefore, this simple scenario is unlikely. Another possible explanation might be the following. As the oscillation amplitude is strongly correlated with the scattering in the system, depleting the bulk carriers might also alter the mobility of the oscillating channel by changing the coupling between the two. From the resistances and Hall measurements at different gate voltages, we indeed find that the mobility increases monotonously from $\sim$830 to 1240 $cm^2/Vs$ when going from $V_g = -10$ V to + 10 V. This behaviour agrees with the expectation that higher mobilities imply less scattering and a reduced broadening of the Landau levels, leading to the increased amplitudes, but the mechanism behind the mobility of the bulk affecting the amplitude of the oscillations in the parallel channel is still not understood and requires additional studies.

The emergence of SdH-oscillations in our measurements of p-doped $Sb_2Te_3$ at magnetic fields $B > 8$ T indicates the presence of a high mobility channel in our system. The signature of multi-channel transport as supported by the nonlinearity of the Hall signal suggests that this channel coexists in parallel to a background channel that does not give rise to oscillations itself. Measurements at different tilt angles reveal that the source channel of the oscillations is a two dimensional system. We can rule out the bulk as the source, since the frequency should be strongly affected by an applied gate voltage, which is not observed while the Hall signal shows clear gate dependence. We therefore conclude that the high mobility channel has to be located at the bottom interface of the film. Although the phase extracted from the Landau level index plot gives no definite proof for quantization of a pure Dirac system, we attribute this to the fact that a straight line fit to our data is too simple to extract the relevant information. A more detailed extraction of the phase with a sophisticated model can be found in the supplementary material. Even though the gate dependence of the oscillation amplitude is not yet fully understood, it stands to reason that it is in some way linked to the interplay between the bulk and the high mobility channel. Exploring this coupling and revealing more information about the origin of the high mobility channel are a promising basis for further experiments.

See supplementary material for further details on MBE-growth and background subtraction as well as an additional analysis of the fan diagram while taking a mixed fermion system (regular and Dirac fermions, including the Zeeman splitting) into account.

The authors are grateful to Gustav Bihlmayer and Martin Lanius for the fruitful discussions and H. Kertz for the technical assistance. This work was supported by the Helmholtz Virtual Institute for Topological Insulators (Jülich-Aachen-Würzburg-Shanghai).

[1] J. E. Moore, Nature **464**, 194 (2010).
[2] M. Z. Hasan and C. L. Kane, Rev. Mod. Phys. **82**, 3045 (2010).
[3] X.-L. Qi and S.-C. Zhang, Phys. Today **63**(1), 33 (2010).
[4] D. Pesin and A. H. MacDonald, Nat. Mater. **11**, 409 (2012).
[5] L. Fu and C. L. Kane, Phys. Rev. Lett. **100**, 096407 (2008).
[6] T. D. Stanescu, J. D. Sau, R. M. Lutchyn, and S. D. Sarma, Phys. Rev. B **81**, 241310 (2010).
[7] D. O. Scanlon, P. D. C. King, R. P. Singh, A. de la Torre, S. M. Walker, G. Balakrishnan, F. Baumberger, and C. R. A. Catlow, Adv. Mater. **24**, 2154 (2012).
[8] P. Lošťák, Z. Starý, J. Horák, and J. Pancíř, Phys. Status Solidi A **115**, 87 (1989).
[9] G. P. Mikitik and Y. V. Sharlai, Phys. Rev. Lett. **82**, 2147 (1999).
[10] J. G. Analytis, J.-H. Chu, Y. Chen, F. Corredor, R. D. McDonald, Z. X. Shen, and I. R. Fisher, Phys. Rev. B **81**, 205407 (2010).
[11] A. A. Taskin, S. Sasaki, K. Segawa, and Y. Ando, Adv. Mater. **24**, 5581 (2012).
[12] L. Fang, Y. Jia, D. J. Miller, M. L. Latimer, Z. L. Xiao, U. Welp, G. W. Crabtree, and W.-K. Kwok, Nano Lett. **12**, 6164 (2012).
[13] Y. Yan, L.-X. Wang, X. Ke, G. Van Tendeloo, X.-S. Wu, D.-P. Yu, and Z.-M. Liao, Sci. Rep. **4**, 3817 (2014).
[14] D.-X. Qu, Y. S. Hor, J. Xiong, R. J. Cava, and N. P. Ong, Science **329**, 821 (2010).
[15] Y. Wang, F. Xiu, L. Cheng, L. He, M. Lang, J. Tang, X. Kou, X. Yu, X. Jiang, Z. Chen, J. Zou, and K. L. Wang, Nano Lett. **12**, 1170 (2012).
[16] X. Yu, L. He, M. Lang, W. Jiang, F. Xiu, Z. Liao, Y. Wang, X. Kou, P. Zhang, J. Tang, G. Huang, J. Zou, and K. L. Wang, Nanotechnology **24**, 015705 (2013).
[17] Z. Ren, A. A. Taskin, S. Sasaki, K. Segawa, and Y. Ando, Phys. Rev. B **82**, 241306 (2010).
[18] J. Xiong, A. Petersen, D. Qu, Y. Hor, R. Cava, and N. Ong, Phys. E **44**, 917 (2012).
[19] J. G. Analytis, R. D. McDonald, S. C. Riggs, J.-H. Chu, G. S. Boebinger, and I. R. Fisher, Nat. Phys. **6**, 960 (2010).
[20] L. Plucinski, A. Herdt, S. Fahrendorf, G. Bihlmayer, G. Mussler, S. Döring, J. Kampmeier, F. Matthes, D. E. Bürgler, D. Grützmacher, S. Blügel, and C. M. Schneider, J. Appl. Phys. **113**, 053706 (2013).
[21] H. Zhang, C.-X. Liu, X.-L. Qi, X. Dai, Z. Fang, and S.-C. Zhang, Nat. Phys. **5**, 438 (2009).
[22] D. Hsieh, Y. Xia, D. Qian, L. Wray, F. Meier, J. H. Dil, J. Osterwalder, L. Patthey, A. V. Fedorov, H. Lin, A. Bansil, D. Grauer, Y. S. Hor, R. J. Cava, and M. Z. Hasan, Phys. Rev. Lett. **103**, 146401 (2009).
[23] Y. Jiang, Y. Wang, M. Chen, Z. Li, C. Song, K. He, L. Wang, X. Chen, X. Ma, and Q.-K. Xue, Phys. Rev. Lett. **108**, 016401 (2012).
[24] M. Lanius, J. Kampmeier, S. Kölling, G. Mussler, P. Koenraad, and D. Grützmacher, J. Cryst. Growth **453**, 158–162 (2016).
[25] Y. Takagaki, A. Giussani, K. Perumal, R. Calarco, and K.-J. Friedland, Phys. Rev. B **86**, 125137 (2012).
[26] A. A. Taskin and Y. Ando, Phys. Rev. B **84**, 035301 (2011).
[27] G. P. Mikitik and Y. V. Sharlai, Phys. Rev. B **85**, 033301 (2012).
[28] A. R. Wright and R. H. McKenzie, Phys. Rev. B **87**, 085411 (2013).
[29] D. Shoenberg, *Magnetic Oscillations in Metals* (Cambridge University Press, 1984).
[30] V. Ariel and A. Natan, in *2013 International Conference on Electromagnetics in Advanced Applications (ICEAA)* (2013), pp. 696–698.
[31] R. Yoshimi, A. Tsukazaki, K. Kikutake, J. G. Checkelsky, K. S. Takahashi, M. Kawasaki, and Y. Tokura, Nat. Mater. **13**, 253 (2014).